Novel diarylamides and diarylureas with *N*-substitution dependent activity against medulloblastoma

Christopher Lawson [a], Thowaiba Babikr Ahmed Alta [b], Georgia Moschou [b],
Vasiliki Skamnaki [c], Theodora G.A. Solovou [c], Caroline Topham [b], Joseph Hayes [a, **],
Timothy J. Snape [a, d, *]

[a] School of Pharmacy and Biomedical Sciences, University of Central Lancashire, Preston, Lancashire, PR1 2HE, UK
[b] School of Science, Engineering and Environment, University of Salford, Salford, M5 4WT, UK
[c] Department of Biochemistry and Biotechnology, University of Thessaly, Biopolis, 41500, Larisa, Greece
[d] Leicester School of Pharmacy, De Montfort University, Leicester, LE1 9BH, UK

ARTICLE INFO

ABSTRACT

Medulloblastoma — highly aggressive and heterogeneous tumours of the cerebellum — account for 15 −20% of all childhood brain tumours, and are the most common high-grade childhood embryonal tumour of the central nervous system. Herein, potent *in vitro* anticancer activity against two established medulloblastoma cell lines of the sonic hedgehog subgroup, namely DAOY (p53 mutant) and ONS-76 (p53 wild type), has been achieved. A number of first-generation diarylamides and diarylureas were evaluated and activity is likely to be, in-part, conformation-dependent. The most active compound from this first-generation set of compounds, 1-naphthyl derivative 4b, was selected and a second-generation of compounds were optimised and tested for activity against the medulloblastoma cell lines. This process resulted in drug-like compounds with up to sixty times the activity (sub-micromolar) of the first-generation — thus providing potent new leads for further study.

1. Introduction

Medulloblastoma are highly aggressive and heterogeneous tumours of the cerebellum that account for 15−20% of all childhood brain tumours, and are the most common high-grade childhood embryonal tumour of the central nervous system. They are most common in children between three and eight years of age, and occur more commonly in males. Symptoms typically include the abrupt onset of headaches, nausea/vomiting, tiredness, loss of balance and coordination, and blurred vision. Surgery remains the initial treatment, followed by whole brain radiotherapy. However, in very young children (less than three years), where whole brain radiotherapy is not recommended, high dose chemotherapy can be given instead (typically combinations of vincristine, cisplatin, lomustine, and cyclophosphamide). Chemotherapy may also be given to children older than three years in addition to radiotherapy [1].

In recent years the molecular and genetic understanding of medulloblastoma has increased dramatically such that it is now possible to classify the disease into four distinct subgroups based on the presence of distinguishing molecular gene signatures: wingless (WNT), sonic hedgehog (SHH), Group 3, and Group 4 [2]. Studies suggest that such stratification confers different clinical outcomes, for example, those in the WNT group have an excellent prognosis while those in Group 3, which are characterised by MYC amplification, fare very poorly, with the other two subgroups having intermediate prognoses. Recently, in 2016, the World Health Organization (WHO) Classification of Tumours of the Central Nervous System acknowledged these subgroups, providing clinical data for the improvement of medulloblastoma diagnosis [3]. However, despite the increasing level of understanding of these subgroupings, relatively few drugs have yet to translate to the clinic against these targets.

---

* Corresponding author. Leicester School of Pharmacy, De Montfort University, Leicester, LE1 9BH, UK.
** Corresponding author.
    E-mail address: tim.snape@dmu.ac.uk (T.J. Snape).

Alongside the ongoing research to identify how these key gene signatures are involved in tumour progression in medulloblastoma, medicinal chemistry approaches must also be used in order to rapidly establish new and better treatments for these patients.

We have an on-going interest in the established phenomenon that diarylamides and diarylureas adopt discrete three-dimensional conformations that place the aromatic rings in either a stacked or unstacked arrangement dependent on their *N*-substitution pattern [4–8], and within the context of cancer therapy, we have previously exploited this through the synthesis of a range of diarylurea-based combretastatin A4 analogues (e.g. 1, Fig. 1). Such compounds possess differing tubulin-binding properties and activities against glioblastoma cell cultures, with the most active compounds mimicking the *Z*-double bond and methoxy substitution pattern of combretastatin A4 [4]. Mimicry of the double bond was achieved through the adoption of a *cis,cis*-conformation upon methylation of the nitrogen atoms thereby placing the aromatic rings in a stacked arrangement. Importantly, the *E*-double bond mimic of the most active compound is the weakest inhibitor of tubulin and gives rise to minimal reduction of proliferation in cell cultures compared to analogues that more closely resemble *Z*-combretastatin A4 in its functionality and three-dimensional structure, features that are mirrored with the *E*- and *Z*-analogues of the natural product itself [4]. Computational studies have identified a possible binding site on the gamma subunit of tubulin (γ-tubulin) for both combretastatin A4 (as its phosphate salt) and colchicine [9], and since poorly differentiated and aggressive brain tumours, for example medulloblastoma, have high levels of γ-tubulin [10], the discovery of a such a binding site on this tubulin subunit offers the possibility of targeting inhibition with new chemotherapeutic agents.

In 2015/16 it was reported that ChEMBL (a database of bioactive molecules with drug-like properties) contained 76,494 urea-derived biologically active molecules, which corresponded to more than 5% of the indexed molecules in total, with the compounds being distributed over all major target classes [11]. Amongst those ureas documented, 34,232 are disubstituted, 39,426 are tri-substituted, but none are tetra-substituted. Given the propensity of diarylureas to adopt different conformations contingent with the *N*-substitution patterns, it is likely that a number of conformational states are possible with these active compounds, but presumably, only one is the active conformation in each case [11].

Based on this likely conformation-dependent activity against numerous biological targets [12–15], we wanted to prepare a series of diarylamides and diarylureas which incorporated the important 3,4,5-trimethoxybenzene ring seen in the majority of classical tubulin inhibitors that bind at the colchicine binding site [16,17], whilst the diaryl amide/urea core itself could potentially bear important complementary binding interactions (Fig. 1) [18]. The methylation status of the amide and urea nitrogen atoms would also create compounds that differed in the conformations adopted, features which appear to be contrasting in tubulin and, say, kinase inhibitors. For example, tubulin's colchicine binding site seems to accept diaryl compounds with a *cis*-arrangement between the aromatic rings [17], whereas kinase inhibitors, as a consequence of only having disubstituted amide/urea nitrogen atoms, tend to prefer a *trans*-arrangement [19], enabling important H-bonds to occur, features which are also presumably possible with the large number of disubstituted urea hits in the ChEMBL database. Conformational differences of the compounds studied herein can be seen in Scheme 1, 3 vs 5 and 4 vs 6.

2. Results and discussion

We began with the synthesis of 28 diarylamides and diarylureas (generation 1), varying in the electron-donating/withdrawing
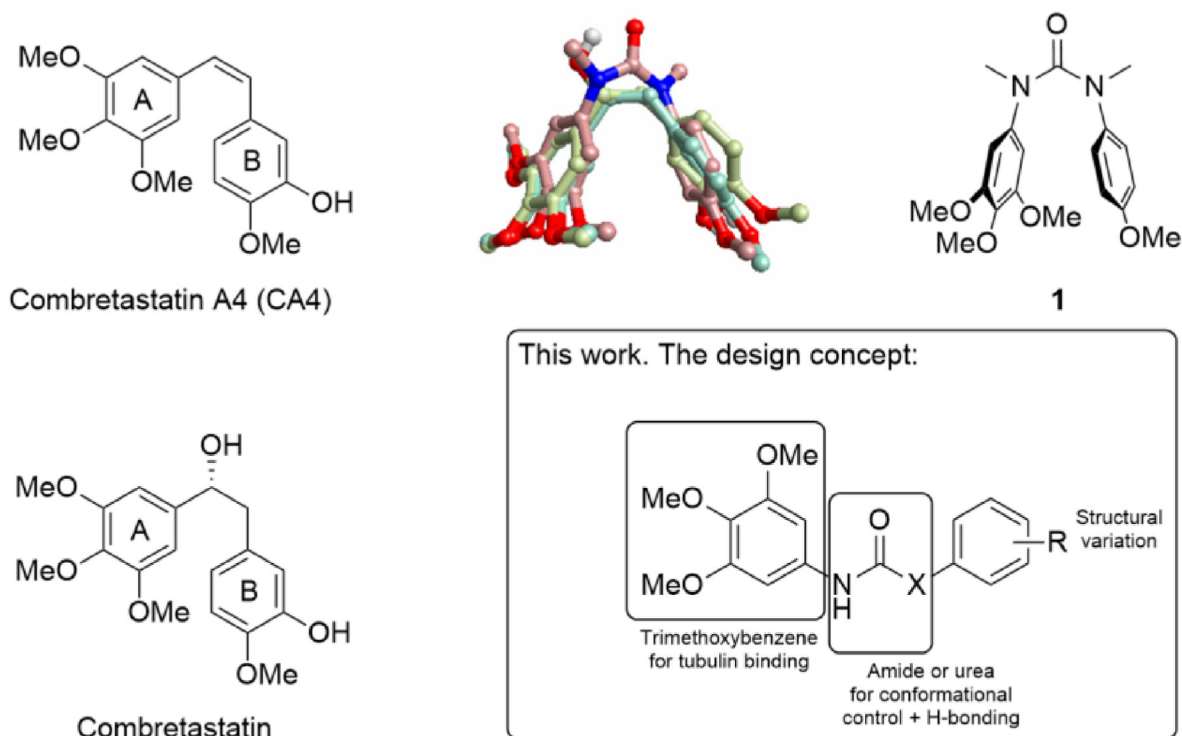

Fig. 1. Combretastatin A4 (top left); a biologically active diarylurea tubulin inhibitor based on the three-dimensional structure of combretastatin A4 (1, top right); and the superposition of combretastatin A-4 (cyan), combretastatin (green, bottom left) and the diarylurea (pink) in the top centre. Structures were aligned using FieldTemplater™ from Cresset BioMolecular Discovery Limited: http://www.cresset-bmd.com/. The design concept for this work is shown in the box.
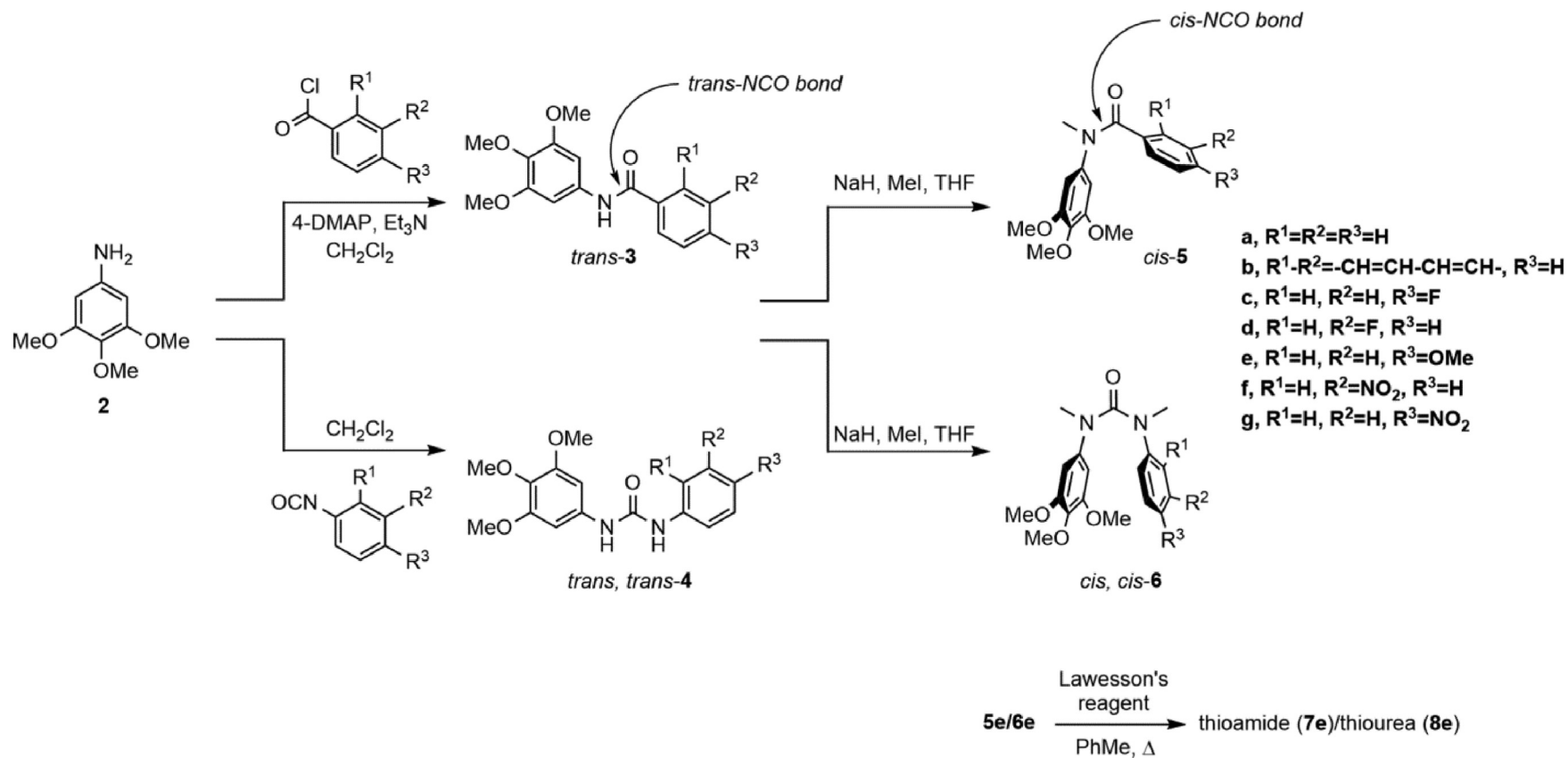
Scheme 1. Synthesis of the compounds tested. All reactions were typically carried out at room temperature and monitored to completion by TLC.

Table 1
IC$_{50}$ values for generation 1 synthesised compounds based on the MTT assay; n = 3; $\geq$125 μM = IC$_{50}$ not determined, as % viability did not drop to 50% at the maximum concentration tested (125 μM). Compounds 4a and 6a were not tested.

Compound	IC$_{50}$ (μM)	
	DAOY cell line (p53 mutant)	ONS76 cell line (p53 wild type)
3a	$\geq$125 μM	$\geq$125 μM
3b	48.71	26.75
3c	$\geq$125 μM	$\geq$125 μM
3d	$\geq$125 μM	$\geq$125 μM
3e	$\geq$125 μM	$\geq$125 μM
3f	$\geq$125 μM	$\geq$125 μM
3g	52.88	$\geq$125 μM
4a	–	–
4b	5.84	2.45
4c	103.8	63.25
4d	111.4	65.55
4e	14.85	12.88
4f	82.48	79.58
4g	70.78	34.98
5a	$\geq$125 μM	$\geq$125 μM
5b	$\geq$125 μM	65.69
5c	$\geq$125 μM	$\geq$125 μM
5d	$\geq$125 μM	$\geq$125 μM
5e	$\geq$125 μM	$\geq$125 μM
5f	$\geq$125 μM	$\geq$125 μM
5g	$\geq$125 μM	$\geq$125 μM
6a	–	–
6b	$\geq$125 μM	$\geq$125 μM
6c	$\geq$125 μM	$\geq$125 μM
6d	$\geq$125 μM	$\geq$125 μM
6e	$\geq$125 μM	$\geq$125 μM
6f	$\geq$125 μM	$\geq$125 μM
6g	$\geq$125 μM	$\geq$125 μM
7e	$\geq$125 μM	85.2
8e	$\geq$125 μM	$\geq$125 μM

nature of the 'B-ring' (Fig. 1), all of which contain the trimethoxybenzene 'A-ring' of combretastatin A4 which has been shown to be crucial to tubulin binding and anticancer activity, by us [4], and others [16]. The N-methylated and non-methylated amides adopt a cis or trans conformation, respectively, whilst the N-methylated and non-methylated ureas adopt a cis,cis or trans, trans conformation, respectively.

2.1. Synthesis

The trans-forms of the amides (3) and ureas (4) were prepared, as depicted in Scheme 1, through the reaction of 3,4,5-trimethoxyaniline (2) and either a substituted benzoyl chloride or arylisocyanate, which was followed by N-methylation to give the cis-forms (5 and 6). Compounds 7e and 8e were synthesised from the corresponding amide or urea using Lawesson's reagent, following standard protocols. Solution-state conformations were confirmed by ^{1}H NMR using the characteristic upfield shift of the aromatic protons which occurs upon stacking in the cis or cis,cis arrangement; Table S1 (see Supporting Information) shows the change in chemical shift ($\Delta\delta$) of the aromatic protons in the trimethoxybenzene ring of all compounds in both conformations. For all methylated compounds, there is the expected upfield shift of the aromatic protons which is consistent with a change in (solution state) conformation and the resultant stacking of the benzene rings (average change in shift, $\Delta\delta = -0.71$). Compounds (3b, 3c, 4d, 6b) were also crystallised and subject to X-ray crystallography and the solid-state conformations matched those expected for both non-methylated and methylated compounds [20].[§]

2.2. Cytotoxicity

With the desired compounds (generation 1) in hand they were subject to a cytotoxicity evaluation using the MTT assay. Two established medulloblastoma cell lines of the sonic hedgehog group, namely DAOY (p53 mutant) and ONS-76 (p53 wild type) were chosen [2], and the IC$_{50}$s can be seen in Table 1.

In general, the amides (both series 3 and 5) were largely inactive, with the exception of the 1-naphthyl analogues (3b and 5b), wherein 3b is active against both cell lines and 5b is active against ONS-76 only, and 3g (p-NO$_2$), which is active against the DAOY cell line only; perhaps suggesting that cell line specificity may be achievable with compounds of this type.

Conversely, there is a stark difference in activity between the ureas (series 4 and 6), with the data showing that all trans,trans-unmethylated compounds (series 4) were active, with the cis,cis-methylated ureas (series 6) being completely devoid of activity over the concentration range and time (0–125 μM, 72h) studied. This difference in activity between the two series is interesting and indicates that both conformation, and/or hydrogen bonding play a role in conferring activity against these medulloblastoma cell lines. In order to try to elucidate the basis of this difference in activity, we used molecular docking calculations with Glide to dock the generation 1 compounds into the colchicine binding site of tubulin (Supporting Information Table S2), and showed that whilst series 4 compounds adopted a trans,trans-conformation in the unbound state and interestingly in the bound state, thus requiring no reorganisational energy, series 6 compounds adopted a cis,cis-conformation in the unbound state (as predicted) but seemed to bind in mixed conformations (either cis,trans or trans, trans) and so, if conformation was important, they would need to overcome conformational energy barriers to bind to tubulin, perhaps explaining their lack of activity here. Whilst previous work by us on tubulin studies with similar N-methylated compounds [4], suggests that cis,cis-conformations do possess inhibition of tubulin polymerisation (23–34% at 10 μM against purified enzyme), presumably by being close structural mimics of combretastatin A4, the levels of inhibition are modest [21].

The thioamide (7e) and thiourea (8e) were interesting inasmuch as only 7e is active (85.2 μM against the ONS-76 cell line) whereas the amide analogue (5e) wasn't, but specifically the sulfur derivatives are inactive, or only weakly so, mirroring their oxygen counterparts.

There was little variation between cell lines overall except for 3g (p-NO$_2$) which exhibited activity against the DAOY cell line only, and 5b (1-naphthyl) and 7e (thioamide) which were selective for the ONS-76 cell line only.

Based on this docking and cytotoxicity data, it appears as though the trans, trans conformation of series 4 compounds is able to mimic the 3-dimensional shape of combretastatin A4. However, despite series 6 also being structurally related, that series of compounds is unable to elicit the same response; presumably a difference related to H-bonding differences or conformational preference. A tubulin polymerisation assay was performed to investigate whether the antiproliferative activities obtained were derived from tubulin binding mechanisms, using both paclitaxel and colchicine as controls (known tubulin inhibitors), however, the tubulin polymerisation results were inconclusive since the compounds failed to significantly inhibit tubulin polymerisation at the concentrations employed. As such, we set out to examine other possible targets of the active compounds (apart from tubulin), and employed further docking studies to consider candidates among various known medulloblastoma protein targets. .

BindingDB, a public, web-accessible database of measured binding affinities [22], was used to provide suggested protein targets known to interact with structurally related diarylurea ligands. In summary, the search with a simple diarylurea (PhNH(CO)NHPh) employing the "substructure" setting resulted in 428 different targets; no hits were obtained if the three methoxy groups were incorporated. The range of targets identified included: multiple kinases (including CDK2, VEGFR2 and Aurora A, >1200 diarylurea hits in total against kinases); angiopoietin-1 receptor; carbonic anhydrase 2; IDH2 (R140Q); integrin α4β1 (VLA-4); mast/stem cell growth factor receptor Kit; mitogen-activated protein kinase 14; platelet-derived growth factor receptors; and numerous purinergic receptors, amongst others.

To identify potential target kinases of interest (given the large (>1200) number of diarylurea hits), all the kinases identified as hits from the database were cross-referenced with kinases known to play a role in brain tumours [23,24]. Based on this data, and structurally similar, known kinase inhibitors, we considered whether the active unmethylated diarylureas (series 4) had the potential to act as kinase type II or type III inhibitors [25]. Therefore, the number of target kinases were filtered even further, and only kinases containing co-complex crystal structures of a bound type II or III ligand were selected for docking.

The first-generation compounds were docked into the five chosen kinases (CDK2; VEGFR2; Aurora A; IGF-1R and B-Raf), to determine whether these compounds could potentially bind. In general, the results indicated that the compounds could bind, and specifically we observed that the *trans, trans* urea 4b was ranked number one against 3 of the 5 kinases studied, and that the unmethylated ureas and amides ranked better than their methylated counterparts.

Having confirmed naphthylamine derivative 4b as a lead compound, a further 56 analogues were designed from commercially available isocyanates containing polycyclic rings with various differentially functionalised groups. Once created, the analogues were prepared for docking against the same kinases utilised for the generation 1 compounds, and eight candidates were selected for synthesis (Table S3). Although we designed the compounds to target kinase inhibition, the 3,4,5-trimethoxyphenyl 'A' ring moiety still remained an integral feature for all generation 2 analogues as some potent kinase inhibitors possess this structure, such as those synthesised by Ganser et al., which exhibit nanomolar activity against VEGFR2 [26].

Once synthesised, the compounds were evaluated for their cytotoxicity, and Table 2 shows the biological activity against both cell lines and the structures of the synthesised compounds and compares the results of these second-generation compounds (9a-9h) against the activity of 4b. Significantly, compounds 9a-9c are an order of magnitude more active than 4b, and almost 60 times more active in the case of naphthol analogue, 9c.

Of note is the improvement in activity of analogue 9c vs 4b by simply incorporating a judiciously placed hydroxyl group; an increase in activity not seen in isomer 9e where, in fact, all activity is lost. Interestingly, any improvement in activity seen by the addition of such an H-bonding group in 9c, is not required in the comparably active indane analogue, 9a. A similar trend is also seen with indole analogues 9b vs 9f where H-bonding and substitution presumably play a large role in conferring activity. Furthermore, the anthracene analogues 9g and 9h again highlight the importance of substitution pattern here since 9h, substituted at position-1, similar to 4b, is active and presumably can reside in the active site of its target, whereas 9g, substituted at position-9, offers a more challenging substrate for the target. On the whole, the most biologically active generation-2 compounds are selective for the DAOY cell line,

confirming their promise as potent lead compounds against (p53 mutant) medulloblastoma cell lines.

Interestingly, despite the promising *in vitro* cytotoxicity data, *in vitro* analysis of the most promising compound (9c) against CDK2, IGF-1R, VEGFR2 and Aurora A kinases [27], only returned ~30% inhibition against Aurora A (at 100 μM), with no notable inhibition against the other kinases, suggesting that these compounds are not potent inhibitors against these kinases but that they exert their effects, at least in part, through interaction with other biological targets.

2.3. ADMET property predictions

To further explore the translational potential of our most active compounds (4b, 9a-d, 9h) from the cellular experiments, ADMET property predictions were performed using the QikProp v5.8 programme [28]. Unfavourable pharmacokinetic profiles are responsible for the failure of many drug candidates [29], with CNS drug development having additional requirements to consider, such as the obstacle of blood-brain barrier (BBB) permeability [30]. Hence, ADMET evaluation earlier in the drug design process is advisable, with computational predictions providing a good starting point. The results of the property predictions are presented in Table 3.

The predicted values should be considered approximate, with some property predictions considerably dependent on conformation. Nevertheless, they provide useful information to be considered in future ligand optimisations. The first test of drug-likeness we looked at was Lipinski's Rule of Five [31]; none of our active compounds demonstrated any violations of these rules. Jorgensen's Rule of Three results were promising with only one of the six compounds, 9h, having a violation [32]. For 9h, a possible solubility issue (log S) was flagged; an obvious consequence of its larger anthracene aromatic substituent. The predicted Caco-2 permeabilities of the compounds are notable, with excellent permeabilities (872−2963 nm s^{-1}) predicted for all compounds. Log BB (logarithmic ratio between concentration of a compound in brain and blood) and CNS values for the compounds are not ideal but exhibit promise for the compounds in further optimisation efforts. A log BB = 0 implies an equal concentration of compound on both sides of the blood brain barrier. The log BB threshold values for blood brain barrier penetration vary in the literature as described in Carpenter et al. [33], and include a log BB value of −1 [34], which suggests that all the compounds pass, but a log BB ≥ 0 is mainly suggested. Additionally, while Veber et al. suggested that a PSA of <140 Å^2 is desirable for oral bioavailability [35], a lower threshold of PSA < 90 Å^2 (and MW < 450 Da) is proposed by van de Waterbeemd for CNS drugs [36]. Estimation of blood-brain barrier crossing of drugs using molecular size and shape, and H-bonding characteristics for drugs targeted to the CNS suggests all compounds fulfil this [36]. The predicted values of logK$_{hsa}$, binding to human serum albumin, for all compounds are within the desired range (−1.5-1.5) for 95% of known drugs. Finally, only compound 9h again raised an initial concern regarding potential blockage of HERG K$^+$ channels. In summary, the most active cellular compounds are also promising CNS drug candidates for lead optimisation considering the predicted pharmacokinetic profiles.

3. Conclusion

To conclude, we have shown that potent anticancer activity has been achieved with a series of diarylureas, primarily against the DAOY medulloblastoma cell line, which represents a disease which is highly aggressive and the most common high-grade childhood embryonal tumour of the central nervous system, but that the

Table 2
IC$_{50}$ values based on the MTT assay; n = 3; $\geq$125 μM = IC$_{50}$ not determined, as % viability did not drop to 50% at the maximum concentration tested (125 μM).

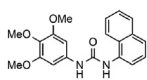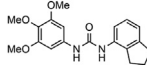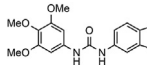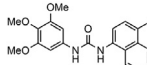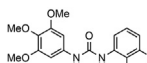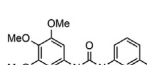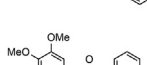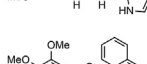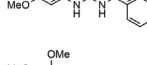| Compound Name	Structure	DAOY cell line (p53 mutant) IC$_{50}$ (μM)	Fold increase: IC$_{50}$ (4b)/IC$_{50}$ [7]	ONS76 cell line (p53 wild type) IC$_{50}$ (μM)	Fold increase: IC$_{50}$ (4b)/IC$_{50}$ [7]
4b		5.84	N/A	2.45	N/A
9a		0.47	12.4	$\geq$125 μM	N/A
9b		0.16	36.5	$\geq$125 μM	N/A
9c		0.10	58.4	2.5	0.98
9d		4.00	1.5	$\geq$125 μM	N/A
9e		$\geq$125 μM	N/A	$\geq$125 μM	N/A
9f		$\geq$125 μM	N/A	$\geq$125 μM	N/A
9g		$\geq$125 μM	N/A	~10	~0.25
9h		1.25	4.7	~10	~0.25

Table 3
Results of ADMET property predictions for selected compounds.[a].

Ligand	Lipinski's Rule of Five and Violations (V)[b]					Jorgensen's Rule of Three and Violations (V)[b]				PSA [Å^2][c]	log K_{hsa}[d]	log BB[e]	CNS	Log HERG (concern below −5)
	M_r [Da]	HBD[f]	HBA[g]	log $P_{(o/w)}$	V	Caco-2 [nm s^{-1}][h]	log S	NPM[i]	V				(-2 − +2)	
	(<500)	($\leq$5)	($\leq$10)	(<5)		(>22)	(>-5.7)	(<7)		(<140 Å^2)				
4b	352.4	2	4.25	3.8	0	2393	−5.1	3	0	68.3	0.2	−0.3	0	−4.8
9a	342.4	2	4.25	3.6	0	2248	−5.1	6	0	69.3	0.3	−0.3	0	−4.2
9b	355.4	2	4.25	3.8	0	2963	−5.1	4	0	70.2	0.2	−0.2	0	−4.5
9c	368.4	3	5	3.1	0	872	−4.7	4	0	89.3	0.1	−0.8	−1	−4.7
9d	353.4	2	5.25	3.2	0	1584	−4.7	4	0	81.0	0.1	−0.5	0	−4.7
9h	402.4	2	4.25	4.8	0	2401	−6.3*	4	1	68.4	0.6	−0.3	0	−5.5*
Range[j]	130−725	0−6	02−20	-2-6.5′	−	<25 poor; > 500 great	−6.5-0.5	1−8	−	7−200	−1.5-1.5	−3.0−1.2		

[a] ADMET data were calculated as described in the text using Qikprop.
[b] Rules as listed in the columns, with any violations of the rules highlighted with an asterisk (*).
[c] PSA represents the van der Waals (polar) surface areas of N and O atoms; recommended PSA <140 Å^2 according to Veber et al..
[d] log K_{hsa}: predicted binding to human serum albumin.
[e] log BB: the predicted blood-brain barrier coefficient.
[f] Number of hydrogen bond donors.
[g] Number of hydrogen bond acceptors.
[h] Caco-2 cell permeability.
[i] Number of primary metabolites.
[j] Range for 95% of known drugs - reference: QikProp version 3.5 User's Manual.

compounds' biological target currently remains elusive. The compounds were identified from a first-generation lead compound (4b), and a second generation of compounds were subsequently designed from it. Further biological testing revealed improved activities (up to 60 times more potent), resulting in new potent (sub-micromolar) lead compounds, with promising ADMET properties, for further study.

Declaration of competing interest

Acknowledgments

Appendix A. Supplementary data

Supplementary data to this article can be found online at https://doi.org/10.1016/j.ejmech.2021.113751.

References

[1] A.M. Martin, E. Raabe, C. Eberhart, K.J. Cohen, Management of pediatric and adult patients with medulloblastoma, Curr. Treat. Options Oncol. 15 (4) (2014 DEC) 581−594.

[2] D.P. Ivanov, B. Coyle, D.A. Walker, A.M. Grabowska, In vitro models of medulloblastoma: choosing the right tool for the job, J. Biotechnol. 236 (2016 OCT 20) 10−25.

[3] D.N. Louis, A. Perry, G. Reifenberger, A. von Deimling, D. Figarella-Branger, W.K. Cavenee, et al., The 2016 World Health organization classification of tumors of the central nervous system: a summary, Acta Neuropathol. 131 (6) (2016 JUN) 803−820.

[4] T.J. Snape, K. Karakoula, F. Rowther, T. Warr, Exploiting conformationally restricted N,N '-dimethyl-N,N '-diarylureas as biologically active C=C double bond analogues: synthesis and biological evaluation of combretastatin A-4 analogues, RSC Adv. 2 (19) (2012) 7557−7560.

[5] Y. Patil-Sen, S.R. Dennison, T.J. Snape, Functional foldamers that target bacterial membranes: the effect of charge, amphiphilicity and conformation, Bioorg. Med. Chem. 24 (18) (2016 SEP 15) 4241−4245.

[6] S. Fahs, F.B. Rowther, S.R. Dennison, Y. Patil-Sen, T. Warr, T.J. Snape, Development of a novel, multifunctional, membrane-interactive pyridinium salt with potent anticancer activity, Bioorg. Med. Chem. Lett 24 (15) (2014 AUG 1) 3430−3433.

[7] S.R. Dennison, T.J. Snape, D.A. Phoenix, Thermodynamic interactions of a cis and trans benzanilide with Escherichia coli bacterial membranes, European Biophysics Journal with Biophysics Letters 41 (8) (2012 AUG) 687−693.

[8] S.R. Dennison, Z. Akbar, D.A. Phoenix, T.J. Snape, Interactions between suitably functionalised conformationally distinct benzanilides and phospholipid monolayers, Soft Matter 8 (11) (2012) 3258−3264.

[9] D.E. Friesen, K.H. Barakat, V. Semenchenko, R. Perez-Pineiro, B.W. Fenske, J. Mane, et al., Discovery of small molecule inhibitors that interact with gamma-tubulin, Chem. Biol. Drug Des. 79 (5) (2012 MAY) 639−652.

[10] V. Caracciolo, L. D'Agostino, E. Draberova, V. Sladkova, C. Crozier-Fitzgerald, D.P. Agamanolis, et al., Differential expression and cellular distribution of gamma-tubulin and beta III-tubulin in medulloblastomas and human medulloblastoma cell lines, J. Cell. Physiol. 223 (2) (2010 MAY) 519−529.

[11] J.R. Loeffler, E.S.R. Ehmki, J.E. Fuchs, K.R. Liedl, Kinetic barriers in the isomerization of substituted ureas: implications for computer-aided drug design, J. Comput. Aided Mol. Des. 30 (5) (2016 MAY) 391−400.

[12] A. Catalano, D. Iacopetta, M.S. Sinicropi, C. Franchini, Diarylureas as antitumor agents, Applied Sciences-Basel 11 (1) (2021 JAN) 374.

[13] Y. Shan, C. Wang, L. Zhang, J. Wang, M. Wang, Y. Dong, Expanding the structural diversity of diarylureas as multi-target tyrosine kinase inhibitors, Bioorg. Med. Chem. 24 (4) (2016 FEB 15) 750−758.

[14] A.R. Abduelkarem, H.S. Anbar, S. Zaraei, A.A. Alfar, O.S. Al-Zoubi, E.G. Abdelkarem, et al., Diarylamides in anticancer drug discovery: a review of pre-clinical and clinical investigations, Eur. J. Med. Chem. 188 (2020 FEB 15), 112029.

[15] D. Strumberg, Preclinical and clinical development of the oral multikinase inhibitor sorafenib in cancer treatment, Drugs Today 41 (12) (2005 DEC) 773−784.

[16] L. Li, S. Jiang, X. Li, Y. Liu, J. Su, J. Chen, Recent advances in trimethoxyphenyl (TMP) based tubulin inhibitors targeting the colchicine binding site, Eur. J. Med. Chem. 151 (2018 MAY 10) 482−494.

[17] W. Li, H. Sun, S. Xu, Z. Zhu, J. Xu, Tubulin inhibitors targeting the colchicine binding site: a perspective of privileged structures, Future Med. Chem. 9 (15) (2017 OCT) 1765−1794.

[18] M.I. El-Gamal, M.A. Khan, H. Tarazi, M.S. Abdel-Maksoud, M.M.G. El-Din, K.H. Yoo, et al., Design and synthesis of new RAF kinase-inhibiting antiproliferative quinoline derivatives. Part 2: diarylurea derivatives, Eur. J. Med. Chem. 127 (2017 FEB 15) 413−423.

[19] J. Dietrich, C. Hulme, L.H. Hurley, The design, synthesis, and evaluation of 8 hybrid DFG-out allosteric kinase inhibitors: a structural analysis of the binding interactions of Gleevec (R), Nexavar (R), and BIRB-796, Bioorg. Med. Chem. 18 (15) (2010 AUG 1) 5738−5748.

[20] C.R. Groom, I.J. Bruno, M.P. Lightfoot, S.C. Ward, The cambridge structural database, Acta Crystallogr. B72 (2016) 171−179, 2016.

[21] M.F. Zayed, H.S. Rateb, S. Ahmed, O.A. Khaled, S.R.M. Ibrahim, Quinazolinone-amino acid hybrids as dual inhibitors of EGFR kinase and tubulin polymerization, Molecules 23 (7) (2018 JUL) 1699.

[22] The Binding Database, https://www.bindingdb.org/bind/index.jsp.

[23] T.J. MacDonald, D. Aguilera, R.C. Castellino, The rationale for targeted therapies in medulloblastoma, Neuro Oncol. 16 (1) (2014 JAN) 9−20.

[24] T.P. Heffron, Challenges of developing small-molecule kinase inhibitors for brain tumors and the need for emphasis on free drug levels, Neuro Oncol. 20 (3) (2018 MAR) 307−312.

[25] R. Roskoski, Classification of small molecule protein kinase inhibitors based upon the structures of their drug-enzyme complexes, Pharmacol. Res. 103 (2016 JAN) 26−48.

[26] C. Ganser, E. Lauermann, A. Maderer, T. Stauder, J.P. Kramb, S. Plutizki, et al., Novel 3-Azaindolyl-4-arylmaleimides exhibiting potent antiangiogenic efficacy, protein kinase inhibition, and antiproliferative activity, J. Med. Chem. 55 (22) (2012 NOV 22) 9531−9540.

[27] The International Centre for Kinase Profiling, http://www.kinase-screen.mrc.ac.uk/.

[28] Release Schrodinger 2018-4, Schrodinger, LLC, New York, NY, 2018.

[29] M.S. Alavijeh, A.M. Palmer, The pivotal role of drug metabolism and pharmacokinetics in the discovery and development of new medicines, Idrugs 7 (8) (2004 AUG) 755−763.

[30] M.S. Alavijeh, M. Chishty, M.Z. Qaiser, A.M. Palmer, Drug metabolism and pharmacokinetics, the blood-brain barrier, and central nervous system drug discovery, NeuroRx 2 (4) (2005) 554−571.

[31] C.A. Lipinski, Drug-like properties and the causes of poor solubility and poor permeability, J. Pharmacol. Toxicol. Methods 44 (1) (2000) 235−249.

[32] W.L. Jorgensen, E.M. Duffy, Prediction of drug solubility from structure, Adv. Drug Deliv. Rev. 54 (1) (2002 MAR 31) 355−366.

[33] T.S. Carpenter, D.A. Kirshner, E.Y. Lau, S.E. Wong, J.P. Nilmeier, F.C. Lightstone, A method to predict blood-brain barrier permeability of drug-like compounds using molecular dynamics simulations, Biophys. J. 107 (3) (2014 AUG 5) 630−641.

[34] J.M. Luco, Prediction of the brain-blood distribution of a large set of drugs from structurally derived descriptors using partial least-squares (PLS) modeling, J. Chem. Inf. Comput. Sci. 39 (2) (1999) 396−404.

[35] D.F. Veber, S.R. Johnson, H.Y. Cheng, B.R. Smith, K.W. Ward, K.D. Kopple, Molecular properties that influence the oral bioavailability of drug candidates, J. Med. Chem. 45 (12) (2002 JUN 6) 2615−2623.

[36] H. van de Waterbeemd, G. Camenisch, G. Folkers, J.R. Chretien, O.A. Raevsky, Estimation of blood-brain barrier crossing of drugs using molecular size and shape, and H-bonding descriptors, J. Drug Target. 6 (2) (1998) 151−165.